Electronic Supplementary Material (ESI) for Journal of Materials Chemistry A.

Supporting information

A study on utilizing different metals as the back contact of $CH_3NH_3PbI_3$ perovskite solar cells

F. Behrouznejad[a], S. Shahbazi[b], N. Taghavinia[a,c]*, Hui-Ping Wu[d], Eric Wei-Guang Diau[d]*

[a]*Institute for Nanoscience and Nanotechnology, Sharif University of Technology, Tehran 14588, Iran.*

[b]*Department of Chemistry, Iran University of Science and Technology, Tehran 1684613114, Iran*
[c]*Department of Physics, Sharif University of Technology, Tehran 14588, Iran Fax: +98-21-66022711; Tel: +98-21-6616 4532; email: taghavinia@sharif.edu.*
[d]*Department of Applied Chemistry and Institute of Molecular Science, National Chiao Tung University, Hsinchu 30010, Taiwan; Fax: +886-3-5723764; Tel: +886-3-5131524; email: diau@mail.nctu.edu.tw.*

Table S1. A comparison of efficiencies of PSCs based on $CH_3NH_3PbI_3$ and different metals as the cathode.

Metal	HTL	Structure	Eff(%)	Stability	Ref
Nano-porous Au (NPG)	_____	FTO/Al_2O_3/$CH_3NH_3PbI_3$/NPG	7.99	____	X. Zhou et al (2015)[10]
Au	Spiro-OMeTAD	FTO/compact TiO2/Li doped TiO_2/ $Cs_5(MA_{0.17}FA_{0.83})(95)Pb(I_{0.83}Br_{0.17})_3$ / Spiro-OMeTAD/Au	21.1	Checked for 250h	M. Saliba et al (2016)[14]
Ag	Spiro-OMeTAD	ITO/ ZnO/ $CH_3NH_3PbI_3$/ Spiro-OMeTAD/ Ag	15.7	____	D. Liu et al (2014)[8]
Embedded Ag mesh in PET (4.3eV)/PH1000(5.08eV)	PEDOT:PSS	Al/PCBM/$CH_3NH_3PbI_3$/PEDOT:PSS/PH1000/Agmesh/PET	14	Checked for 500h:13.5% to 12%	Y. Li et al (2016)[7]
AgAl alloy	Spiro-OMeTAD	FTO/ TiO_2/$CH_3NH_3PbI_{3-x}Cl_x$/ SpiroOMeTAD	11.07	____	Y. Luo et al (2015)[15]
Ni	Spiro-OMeTAD	FTO/TiO_2(rutile)/$CH_3NH_3PbI_3$/Spiro/Ni	10.40	Checked for 5days.	Q. Jiang (2014)[1]
Ni	NiO	FTO/TiO_2/$CH_3NH_3PbI_{3-x}Cl_x$/NiO	7.28	Checked for 60 days	B. Abdollahi (2015)[12]
Ni mesh embedded in PET/PEDOT:PSS/ silver-free transparent con- ducting adhesive(TCA)	SpiroOMeTad	FTO/ Al_2O_3/ $CH_3NH_3PbI_{3-x}Cl_x$/ SpiroOMeTad/ Ni mesh embedded in PET/PEDOT:PSS	13.3	____	D. Bryant (2014)[16]
Mo	SpiroOMeTad	FTO/TiO_2(rutile)/$CH_3NH_3PbI_3$/SpiroOMeTad/Mo	15.06	____	J. Jeong et al (2015)[11]
Cu	____	____	____	____	____
Pt	____	____	____	____	____
Cr	____	____	____	____	____
C (Laminated carbon nanotubes)	____	FTO/ TiO2/ $CH_3NH_3PbI_3$/ CNT film	6.87		Z. Li et al (2014)[17]
C (candle soot)	____	FTO/ TiO2/ $CH_3NH_3PbI_3$ / C	9.78		Z. Wei et al (2014)[18]

Table S2. A comparison of efficiencies of PSCs based on $CH_3NH_3PbI_3$ and different metals as the anode.

Metal	ETL	structure	Eff(%)	Ref
Al	$PC_{61}BM$	ITO/PEDOT:PSS/$CH_3NH_3PbI_3$/$PC_{61}BM$/Al	5.2	S. Sun et al (2014)[9]
Ag	$PC_{61}BM$	ITO/PEDOT:PSS/p-type interlayer/perovskite/PC60BM/ LiF/Ag	15.2	Q. Lin et al (2015)[6]
Ag	$PC_{61}BM$/ C_{60}-bis	ITO/PEDOT:PSS/ perovskite/$PC_{60}BM$/ C_{60}-bis/Ag	11.65	D. Wang et al (2014)[19]
Cu		Cu/ ETL/ $FA_xMA_{1-x}PbI_3$/ HTL/ ITO	18	Y. Deng et al (2016)[20]

Table S3. Photovoltaic characteristics of HTM-free PSCs with Ag as a back contact metal.

Ag-Sample number	A(cm²)	Jsc	Voc	FF	eff
Ag-1	0.09	3.19	0.042	30.10	0.04
Ag-2	0.09	3.76	0.072	39.84	0.11
Ag-3	0.09	4.931	0.087	39.34	0.17
average		3.96	0.067	36.42	0.11
$S(standard\ deviation) = \sqrt{\frac{\sum_1^N (x-\bar{x})^2}{(N-1)}}$		0.89	0.023	5.49	0.07

Table S4. Photovoltaic characteristics of PSCs with spiro OMeTAD as a HTM. Ag is used as a back contact metal.

Ag/spiro-Sample number	A(cm²)	Jsc	Voc	FF	eff
Ag-HTM-1	0.09	20.60	1.023	78.32	16.51
Ag-HTM-2	0.09	20.27	1.015	78.28	16.10
Ag-HTM-3	0.09	20.73	1.009	77.14	16.14
average		20.53	1.016	77.91	16.25
$S(standard\ deviation) = \sqrt{\frac{\sum_1^N (x-\bar{x})^2}{(N-1)}}$		0.24	0.007	0.67	0.23

Table S5. Photovoltaic characteristics of HTM-free PSCs with Cr as a back contact metal.

Cr-Sample number	A(cm^2)	Jsc	Voc	FF	eff
Cr-1	0.09	0.89	0.753	21.83	0.14
Cr-2	0.09	0.71	0.801	18.90	0.11
Cr-3	0.09	0.93	0.559	22.16	0.12
average		0.84	0.704	20.96	0.12
$S(standard\ deviation) = \sqrt{\frac{\sum_1^N (x-\bar{x})^2}{(N-1)}}$		0.12	0.128	1.79	0.015

Table S6. Photovoltaic characteristics of PSCs with spiro OMeTAD as a HTM. Cr is used as a back contact metal.

Cr/spiro-Sample number	A(cm^2)	Jsc	Voc	FF	eff
Cr-HTM-1	0.09	0.25	0.858	20.35	0.04
Cr-HTM-2	0.09	0.494	0.632	14.82	0.05
Cr-HTM-3	0.09	0.475	0.688	15.25	0.05
average		0.406	0.726	12.47	0.05
$S(standard\ deviation) = \sqrt{\frac{\sum_1^N (x-\bar{x})^2}{(N-1)}}$		0.136	0.118	3.07	0.006

Table S7. Photovoltaic characteristics of HTM-free PSCs with Ag as a back contact metal.

Cu-Sample number	A(cm²)	Jsc	Voc	FF	eff
Cu-1	0.09	4.326	0.231	21.02	0.21
Cu-2	0.09	10.42	0.301	33.69	1.06
Cu-3	0.09	7.72	0.279	27.82	0.6
Cu-4	0.09	7.07	0.159	26.08	0.29
Cu-5	0.09	6.83	0.201	42.95	0.59
average		7.27	0.234	30.31	0.55
$S(standard\ deviation) = \sqrt{\frac{\sum_1^N (x-\bar{x})^2}{(N-1)}}$		2.18	0.058	8.39	0.33

Table S8. Photovoltaic characteristics of PSCs with spiro OMeTAD as a HTM. Cu is used as a back contact metal.

Cu/spiro-Sample number	A(cm²)	Jsc	Voc	FF	eff
Cu-HTM-1	0.09	20.32	0.942	47.89	9.17
Cu-HTM-2	0.09	20.97	0.905	45.12	8.56
Cu-HTM-3	0.09	21.17	0.867	46.69	8.57
Cu-HTM-4	0.09	17.66	0.945	52.06	8.68
Cu-HTM-5	0.09	17.28	0.940	55.34	8.99
average		19.48	0.920	49.42	8.79
$S(standard\ deviation) = \sqrt{\frac{\sum_1^N (x-\bar{x})^2}{(N-1)}}$		1.87	0.03	4.19	0.27

Table S9. Photovoltaic characteristics of HTM-free PSCs with Ni as a back contact metal.

Ni-Sample number	A(cm²)	Jsc	Voc	FF	eff
Ni-1	0.09	9.03	0.421	44.39	1.69
Ni-2	0.09	8.52	0.411	49.92	1.75
Ni-3	0.09	9.56	290	41.26	1.15
Ni-4	0.09	8.06	324	47.38	1.24
Ni-5	0.09	10.04	335	44.37	1.49
average		9.04	0.356	45.46	1.46
$S(standard\ deviation) = \sqrt{\frac{\sum_1^N (x-\bar{x})^2}{(N-1)}}$		0.79	0.057	3.3	0.27

Table S10. Photovoltaic characteristics of PSCs with spiro OMeTAD as a HTM. Ni is used as a back contact metal.

Ni/spiro-Sample number	A(cm²)	Jsc	Voc	FF	eff
Ni-HTM-1	0.09	18.89	0.900	40.79	6.93
Ni-HTM-2	0.09	18.02	0.711	55.64	7.13
Ni-HTM-3	0.09	18.21	0.834	51.61	7.83
average		18.37	0.815	49.35	7.30
$S(standard\ deviation) = \sqrt{\frac{\sum_1^N (x-\bar{x})^2}{(N-1)}}$		0.46	0.096	7.68	0.47

Table S11. Photovoltaic characteristics of HTM-free PSCs with Pt as a back contact metal.

Pt-Sample number	A(cm²)	Jsc	Voc	FF	eff
Pt-1	0.09	7.17	0.686	62.6	3.08
Pt-2	0.09	7.22	0.667	63.26	3.04
Pt-3	0.09	6.62	0.647	61.51	2.63
average		7.00	0.67	62.46	2.92
$S(standard\ deviation) = \sqrt{\frac{\sum_1^N (x-\bar{x})^2}{(N-1)}}$		0.33	0.02	0.88	0.25

Table S12. Photovoltaic characteristics of PSCs with spiro OMeTAD as a HTM. Pt is used as a back contact metal.

Pt/spiro-Sample number	A(cm²)	Jsc	Voc	FF	eff
Pt-HTM-1	0.09	20.36	1.009	69.84	14.35
Pt-HTM-2	0.09	20.58	1.006	71.07	14.72
Pt-HTM-3	0.09	20.48	1.003	70.35	14.45
average		20.47	1.006	70.42	14.51
$S(standard\ deviation) = \sqrt{\frac{\sum_1^N (x-\bar{x})^2}{(N-1)}}$		0.11	0.003	0.62	0.19

Table S13. Photovoltaic characteristics of HTM-free PSCs with Au as a back contact metal.

Au-Sample number	A(cm^2)	Jsc	Voc	FF	eff
Au-1	0.09	4.94	0.739	65.71	2.40
Au-2	0.09	4.85	0.809	65.38	2.56
Au-3	0.09	5.47	0.747	58.72	2.40
Au-4	0.09	8.05	0.506	60.35	2.46
average		5.83	0.700	62.54	2.46
$S(standard\ deviation) = \sqrt{\frac{\sum_1^N (x-\bar{x})^2}{(N-1)}}$		1.51	0.130	3.54	0.08

Table S14. Photovoltaic characteristics of PSCs with spiro OMeTAD as a HTM. Au is used as a back contact metal.

Au/spiro-Sample number	A(cm^2)	Jsc	Voc	FF	eff
Au-HTM-1	0.09	21.21	1.003	76.83	16.35
Au-HTM-2	0.09	20.99	1.009	77.60	16.44
average		21.21	1.006	77.22	16.40
$S(standard\ deviation) = \sqrt{\frac{\sum_1^N (x-\bar{x})^2}{(N-1)}}$		0.16	0.004	0.54	0.06

Table S15. A comparison of electron affinity and work-function of perovskite layer in different structures of PSC.

a	ETL or HTL	Structure	Electron affinity (eV)	Work-function (eV)	Eg (eV)	ref	Method
Si	TiO_2: Electron affinity: 4.1eV Work-function: 4.65eV Eg: 3.2eV	Si/TiO_2/$CH_3NH_3PbI_3$	3.9	4.8	1.55	A. Dymshits et al (2015)[22]	Kelvin probe force microscopy (KPFM)
ITO	_____	ITO/$CH_3NH_3PbI_3$		4.5		K. G. Lim et al (2016)[23]	ultraviolet photoelectron spectroscopy (UPS)
ITO	PEDOT:PSS	ITO/PEDOT:PSS / $CH_3NH_3PbI_3$		5.01		K. G. Lim et al (2016)[23]	UPS
Au	____	Au/ $CH_3NH_3PbI_3$	4.0	4.7	1.7	X. Liu et al (2015)[24]	UPS/IPES
FTO	Cu_2O	FTO/ /Cu_2O/$CH_3NH_3PbI_3$	4.1	4.9	1.7	E. M. Miller et al (2014)[21]	XPS
FTO	NiO	FTO/compact TiO_2/$CH_3NH_3PbI_3$	3.82	4.49	1.7	E. M. Miller et al (2014)[21]	XPS
ITO	PEDOT:PSS	ITO/ PEDOT:PSS /$CH_3NH_3PbI_3$	4.11	4.43	1.7	E. M. Miller et al (2014)[21]	XPS
FTO	____	FTO/compact TiO_2/$CH_3NH_3PbI_3$	4.21	4.22	1.7	E. M. Miller et al (2014)[21]	XPS
FTO	Al_2O_3	FTO/compact TiO_2/$CH_3NH_3PbI_3$	3.72	3.72	1.7	E. M. Miller et al (2014)[21]	XPS
FTO	ZnO	FTO/compact TiO_2/$CH_3NH_3PbI_3$	4.66	4.64	1.7	E. M. Miller et al (2014)[21]	XPS
FTO	TiO_2	FTO/compact TiO_2/$CH_3NH_3PbI_3$	4.05	4.03	1.7	E. M. Miller et al (2014)[21]	XPS
FTO	ZrO_2	FTO/compact TiO_2/$CH_3NH_3PbI_3$	3.93	3.86	1.7	E. M. Miller et al (2014)[21]	XPS

Fig. S1 Energy diagram of FTO/TiO_2/$CH_3NH_3PbI_3$/metal structure with Ag as the back electrode (simulated by Scaps software in the dark condition). Three work-functions for isolated $CH_3NH_3PbI_3$ are investigated: 4.65eV, 4.15eV and 5.15 eV in case of considering it as an intrinsic, n-type and p-type semi-conductor. There is no significant change due to the low effective mass of electron and hole in its structure.

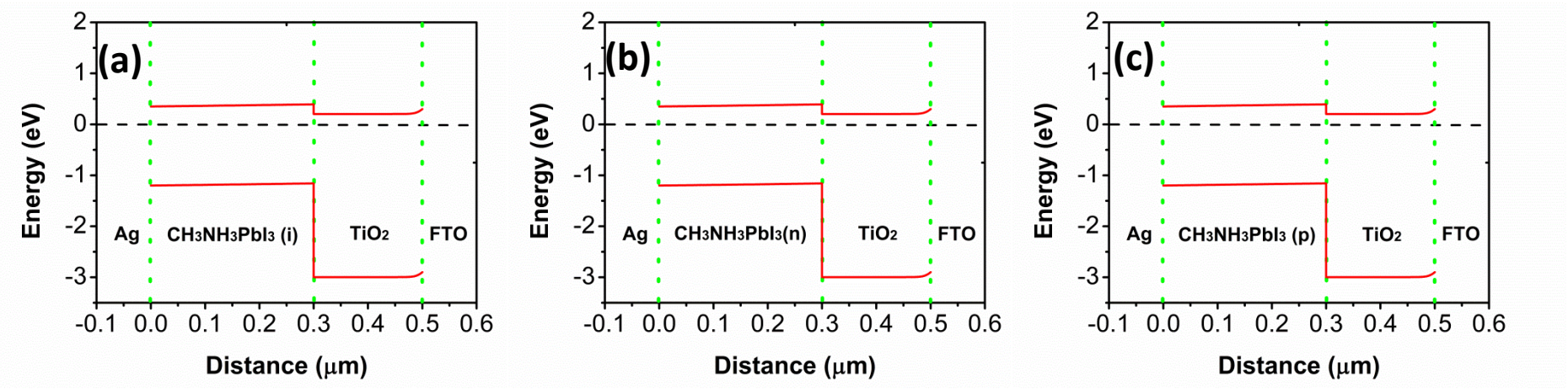

Fig. S2 Energy diagram of FTO/TiO_2/$CH_3NH_3PbI_3$/metal structure with Cu as the back electrode (simulated by Scaps software in the dark condition). Three work-functions for isolated $CH_3NH_3PbI_3$ are investigated: 4.65eV, 4.15eV and 5.15 eV in case of considering it as an intrinsic, n-type and p-type semi-conductor. There is no significant change due to the low effective mass of electron and hole in its structure.

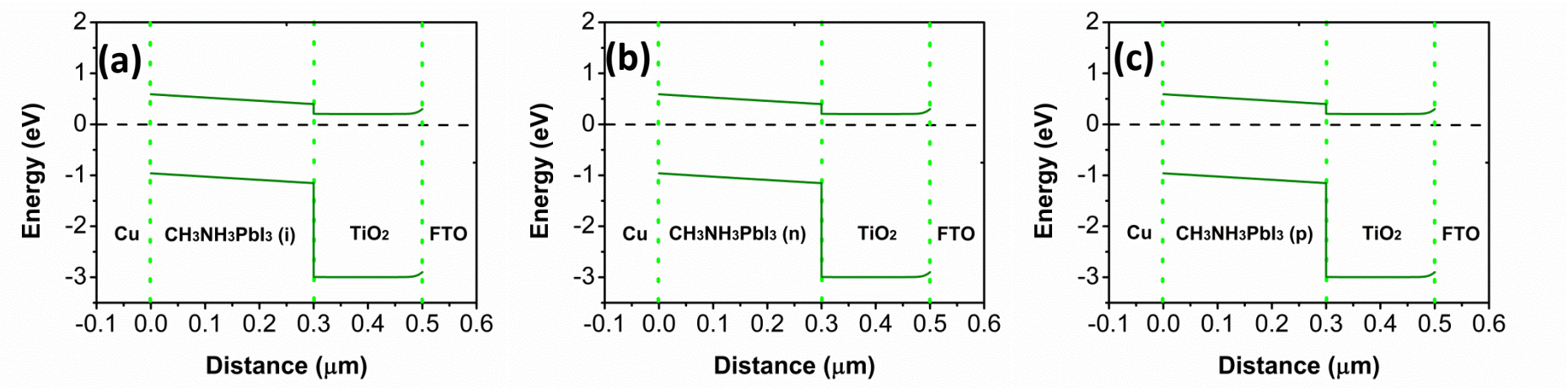

Fig. S3 Energy diagram of FTO/TiO_2/$CH_3NH_3PbI_3$/metal structure with Cr as the back electrode (simulated by Scaps software in the dark condition). Three work-functions for isolated $CH_3NH_3PbI_3$ are investigated: 4.65eV, 4.15eV and 5.15 eV in case of considering it as an intrinsic, n-type and p-type semi-conductor. There is no significant change due to the low effective mass of electron and hole in its structure.

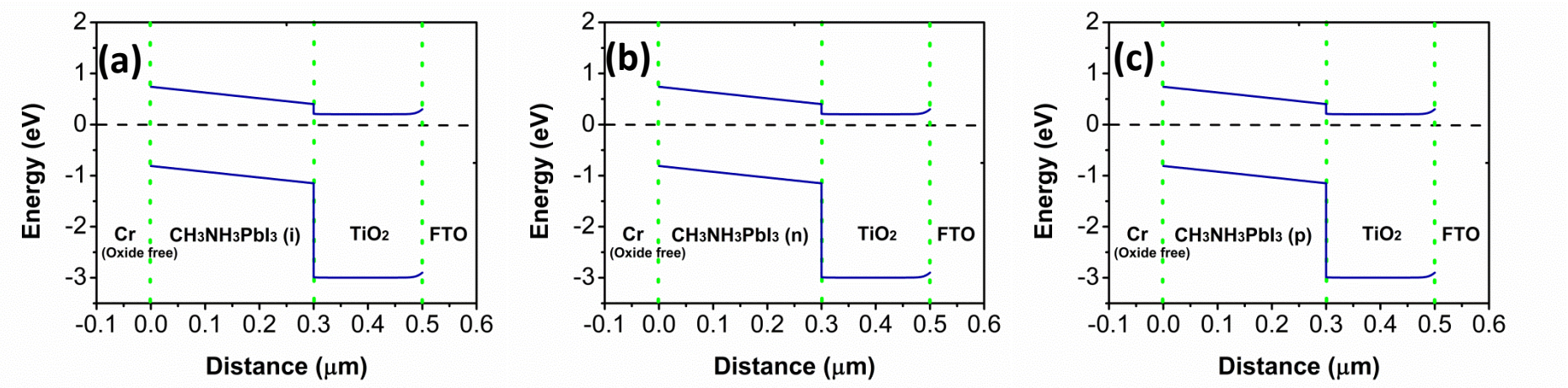

Fig. S4 Energy diagram of FTO/TiO_2/$CH_3NH_3PbI_3$/metal structure with Au as the back electrode (simulated by Scaps software in the dark condition). Three work-functions for isolated $CH_3NH_3PbI_3$ are investigated: 4.65eV, 4.15eV and 5.15 eV in case of considering it as an intrinsic, n-type and p-type semi-conductor. There is no significant change due to the low effective mass of electron and hole in its structure.

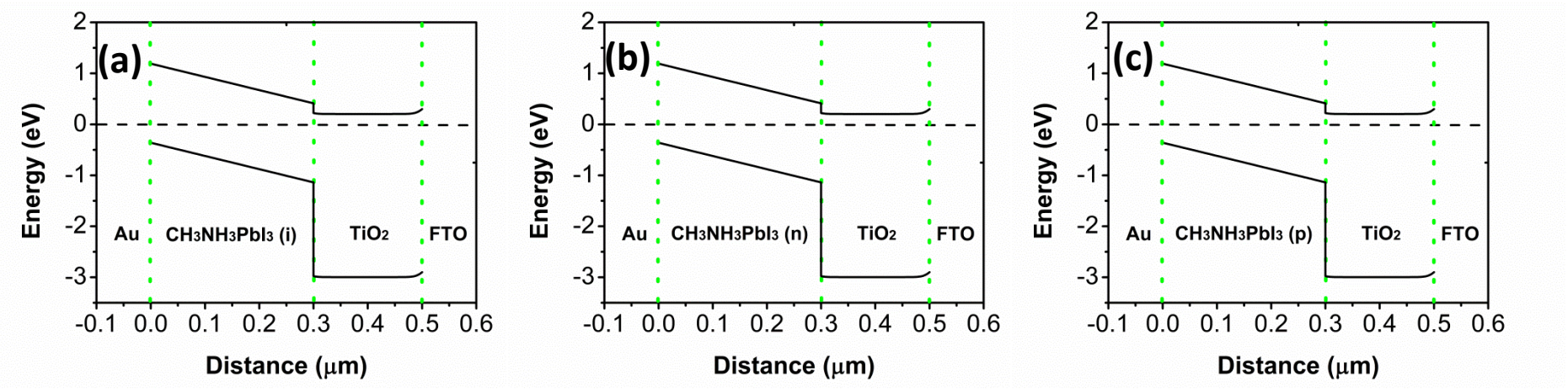

Fig. S5 Energy diagram of FTO/TiO_2/$CH_3NH_3PbI_3$/metal structure with Pt as the back electrode (simulated by Scaps software in the dark condition). Three work-functions for isolated $CH_3NH_3PbI_3$ are investigated: 4.65eV, 4.15eV and 5.15 eV in case of considering it as an intrinsic, n-type and p-type semi-conductor. There is no significant change due to the low effective mass of electron and hole in its structure.

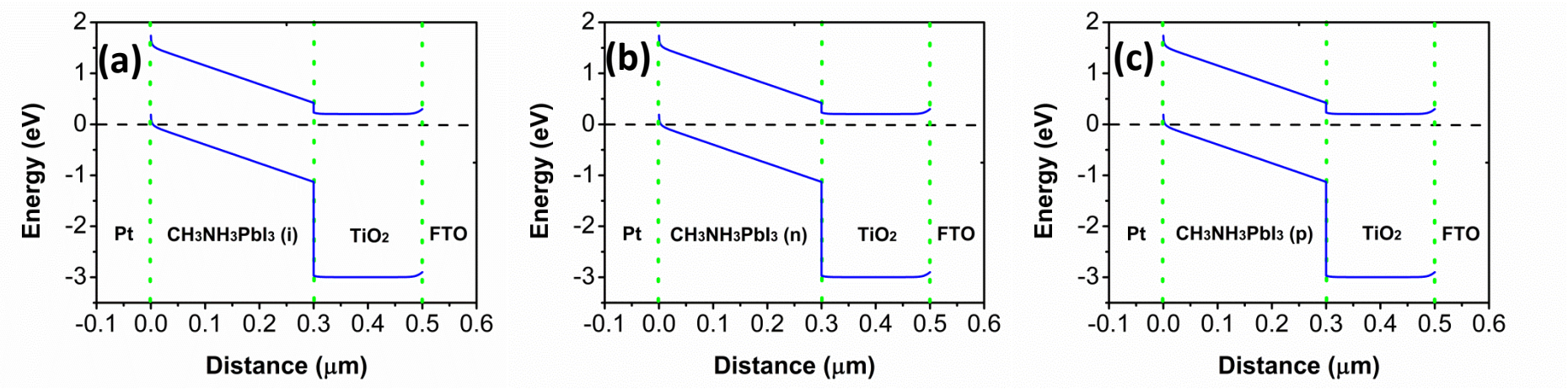

Fig. S6 Images of PSCs with Ag as a back contact in HTM-free PSCs from back side, a few days after deposition (a) and three months after deposition (e). As indicated, the absorber layer is completely discoloured a few days after deposition and after three months Ag layer is also degraded considerably. The image from front side is shown in fig (c). Fig b, d & f show PSC with spiro OMeTAD as a hole transporter from back side a few days after deposition, front side after three months and back side after three months. In these images the yellow color of AgI is more distinguishable. Probably the HTM layer protects AgI from photo-decomposition to some extent.

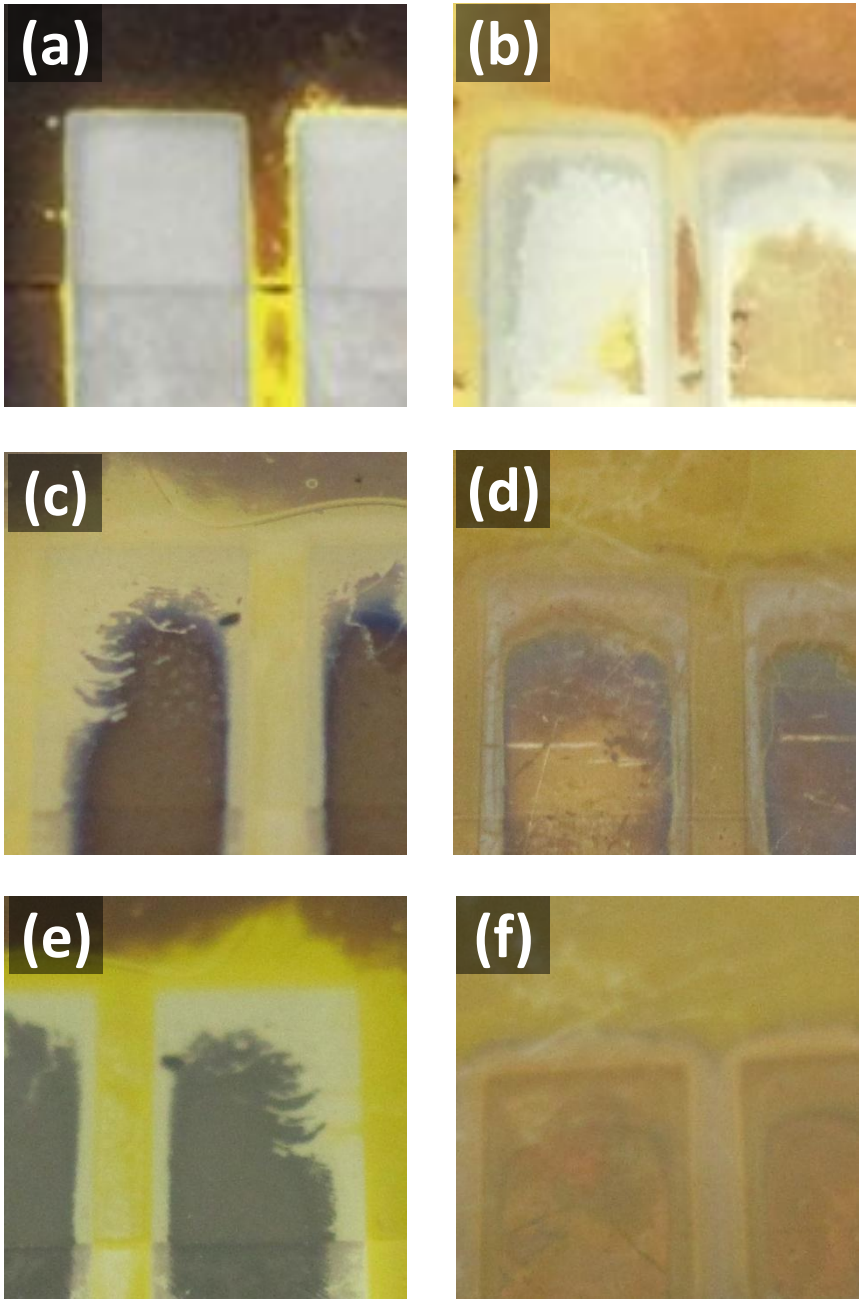

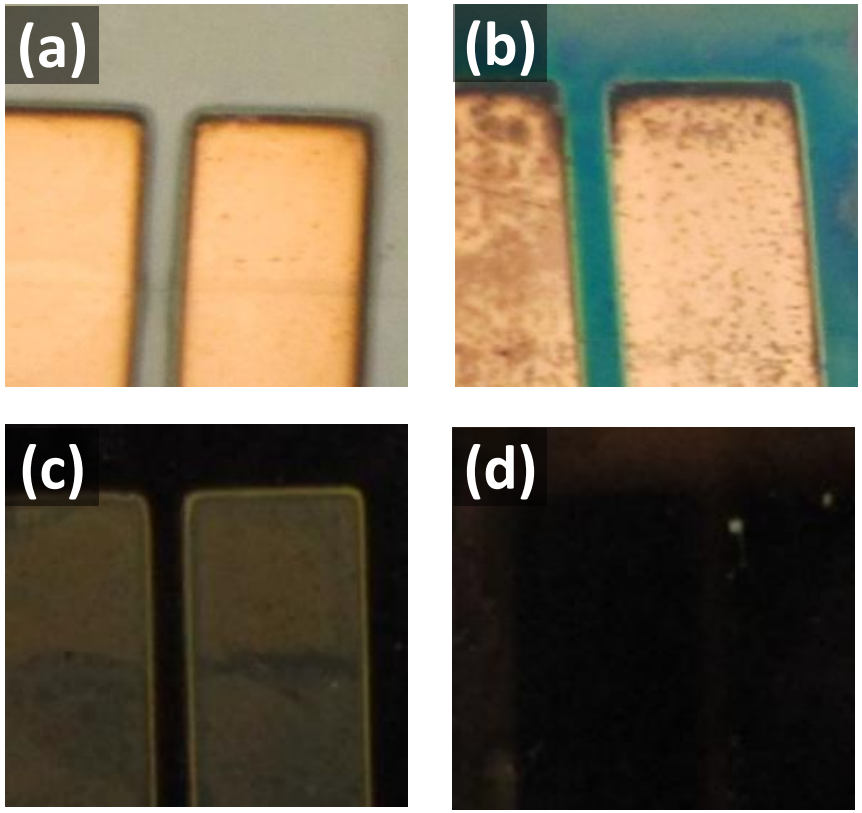

Fig. S7 Images from front (a) and back-side (c) of HTM-free PSCs with Cu as a contact metal in comparison with PSCs with spiro-OMeTAD as a HTM from front (b) and back-side (d). The images are taken three months after fabrication. The absorber layer is almost discoloured in HTM-free device due to CuI formation (c), but the HTM layer protects it to some extent (d).

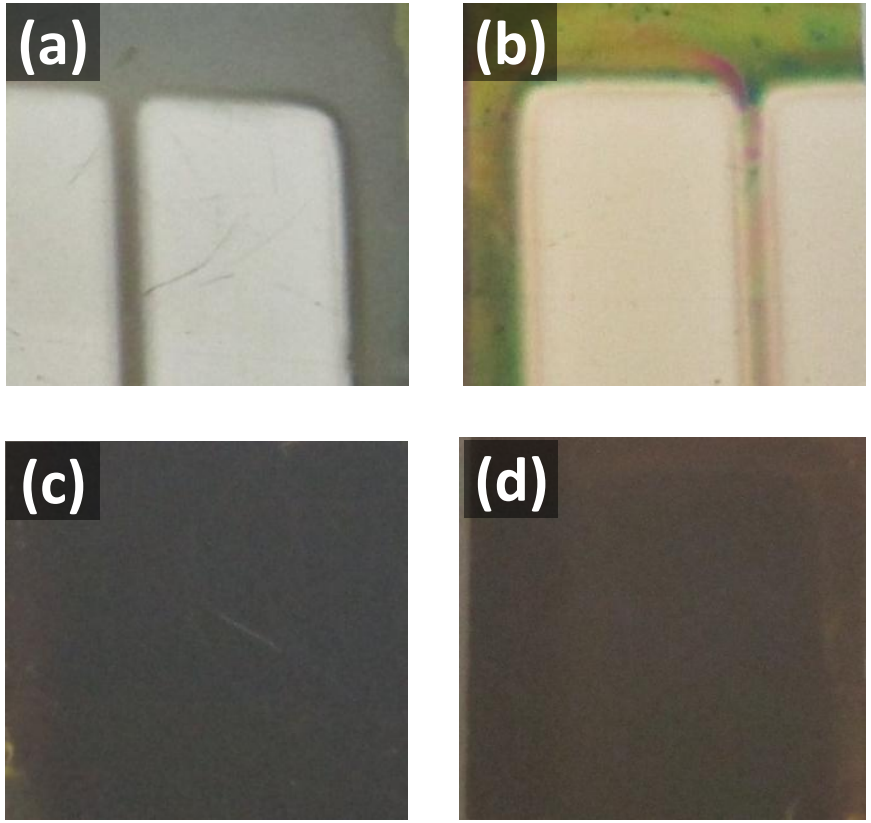

Fig. S8 Images from front (a) and back-side (c) of HTM-free PSCs with Cr as a contact metal in comparison with PSCs with spiro-OMeTAD as a HTM from front (b) and back-side (d). The images are taken three months after fabrication. The color of absorber layer does not change significantly. It seems that Cr does not enter any chemical reactions with $CH_3NH_3PbI_3$ or HTM layers.

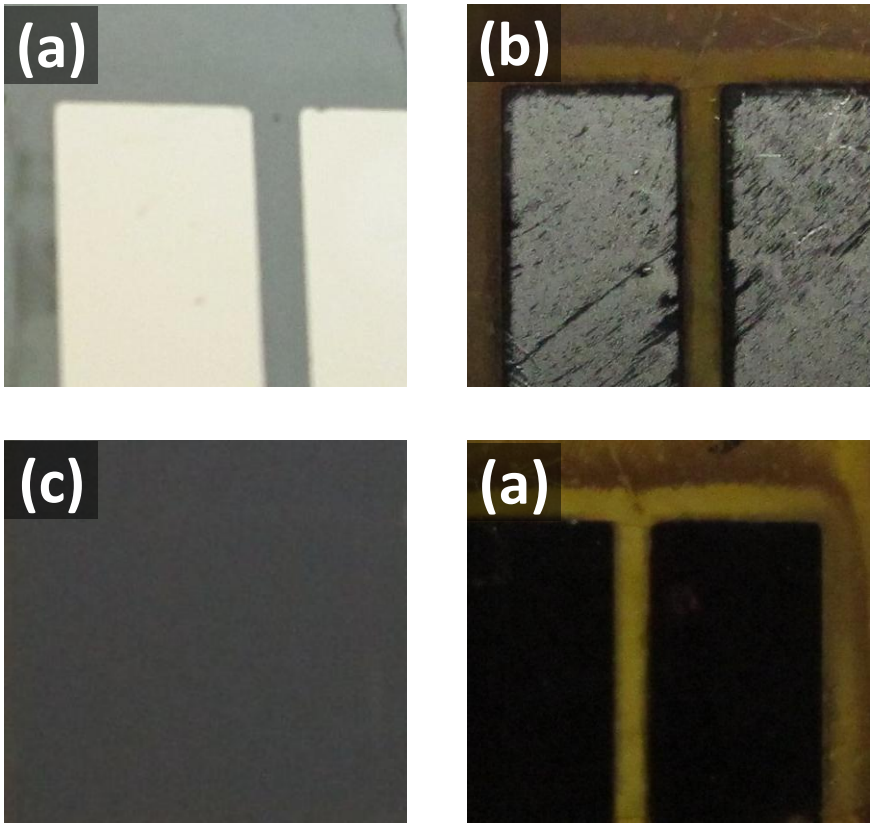

Fig. S9 Images from front (a) and back-side (c) of HTM-free PSCs with Pt as a contact metal in comparison with PSCs with spiro-OMeTAD as a HTM from front (b) and back-side (d). The images are taken three months after fabrication. The color of absorber layer at the back of Pt thin film does not change significantly. It seems that Pt does not enter any chemical reactions with $CH_3NH_3PbI_3$ or HTM layers.

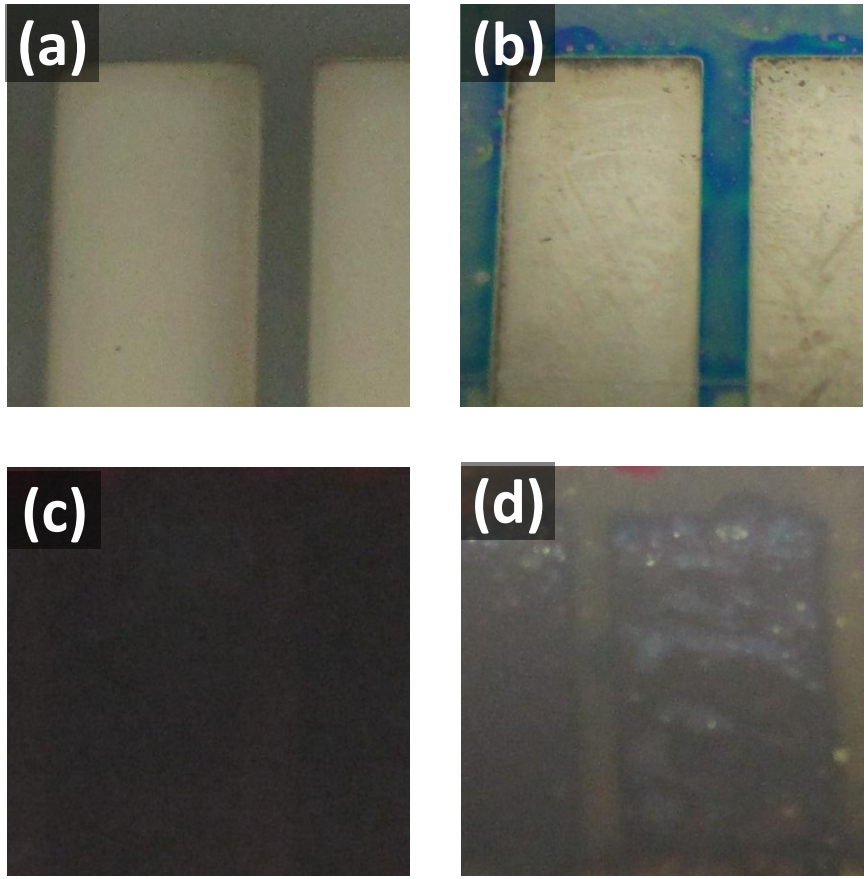

Fig. S10 Images from front (a) and back-side (c) of HTM-free PSCs with Ni as a contact metal in comparison with PSCs with spiro-OMeTAD as a HTM from front (b) and back-side (d). The images are taken three months after fabrication. The color of absorber layer at the back of Ni thin film does not change significantly. It seems that Ni does not enter any chemical reactions with $CH_3NH_3PbI_3$, but it is not compatible with spiro-OMeTAD layer as shown in (d).

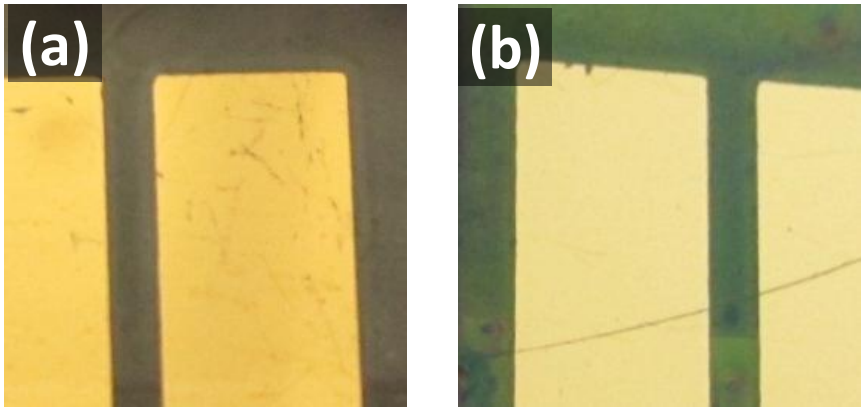

Fig. S11 Images from front side of HTM-free PSC (a) and PSC with spiro-OMeTAD as a HTM (b). Au thin film is deposited as a back contact material. The images are taken three months after fabrication. The colour of absorber layer does not change significantly due to chemical stability of Au layer.

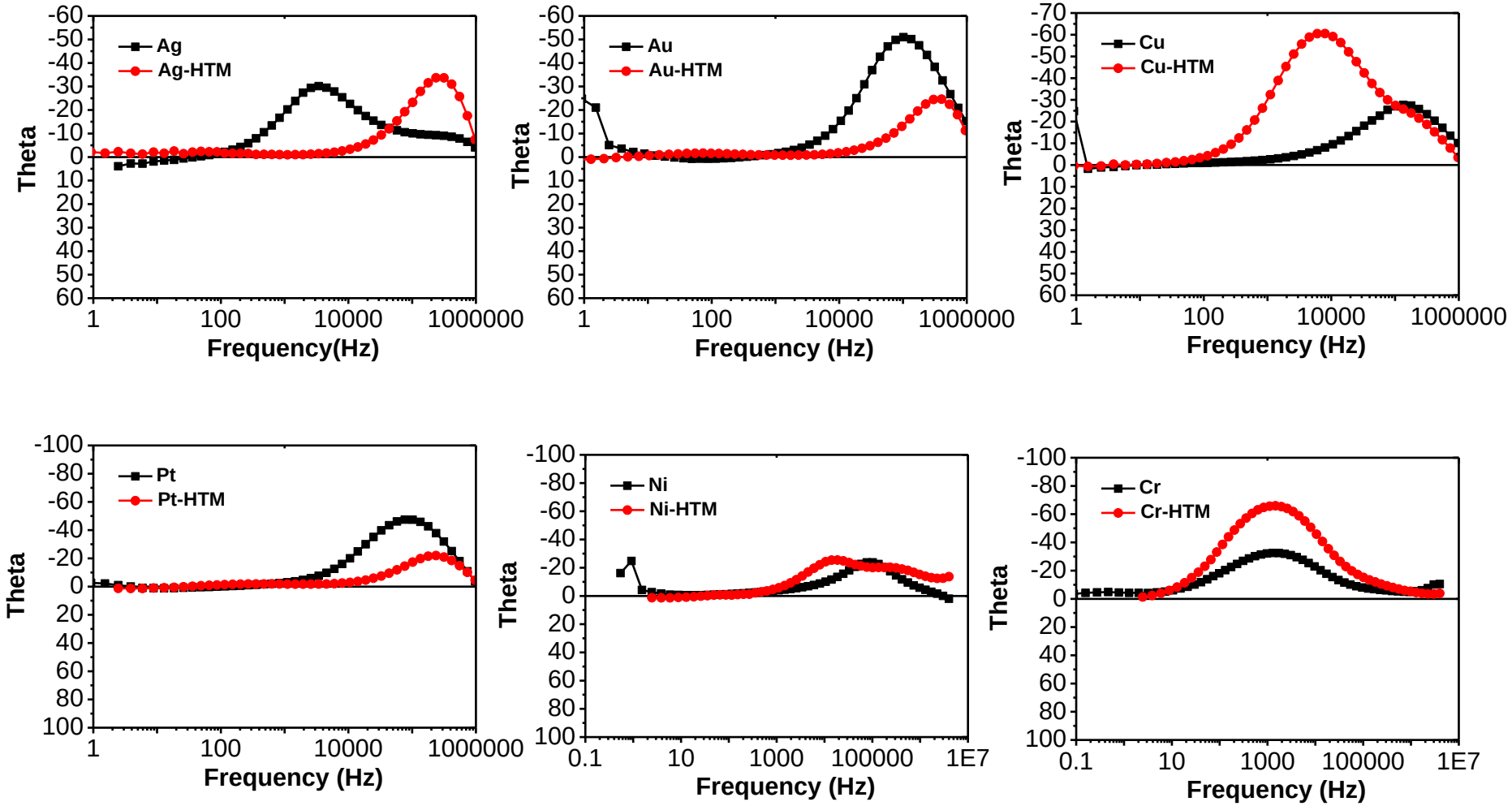

Fig. S7 Bode plots for HTM-free PSCs with Pt, Au, Ni, Cu, Cr and Ag as a back contact electrode in comparison with PSCs utilizing spiro-OMeTAD as HTM. HTM represents spiro-OMeTAD.

Table S16 Fitting results related to nyquist plots that are reported in Fig. 4.

Sample	R_s(Ω.. cm^2(	R_{ct1}(Ω.. cm^2)	T_1	P_1	C_1 (F.cm-2)	R_{ct2}(Ω..cm^2(	T_2	P_2	C_2 (F.cm-2)
Au	3.0	25.0	2.8E-7	0.97	1.94E-7	_____	_____	_____	_____
Ag	2.6	1.5	5E-6	0.85	6.23E-7	_____	_____	_____	_____
Pt	3.2	24.0	5.2E-7	0.94	2.52E-7	_____	_____	_____	_____
Ni	8.2	9.0	4E-7	0.97	2.71E-7	9.3	8E-5	0.65	1.65E-6
Cu	8.3	26.5	1.4E-6	0.8	1.09E-7	1.5	0.0004	0.9	0.00018
Cr	45.0	6.0	1E-6	0.8	4.95E-8	435	1.7E-5	0.665	1.44E-6
Au-HTM	1.55	2.77	7E-7	0.93	2.60E-7	0.45	0.03	0.7	0.0047
Ag-HTM	1.9	5.1	3E-7	0.98	2.28E-7	_____	_____	_____	_____
Pt-HTM	3.75	5.2	3E-7	0.94	1.28E-7	0.8	0.002	0.85	0.00064
Ni-HTM	31.0	30.0	9E-8	0.897	2.06E-8	_____	_____	_____	_____
Cu-HTM	5.5	6.0	8E-6	0.8	6.66E-7	155	1E-6	0.97	7.62E-7
Cr-HTM	24.6	24.6	1E-6	0.88	2.35E-7	2140	1.5E-6	0.87	6.36E-7

A description about relativistic effects on diffuse reflectance of different metals (related to Fig 6-a):

The yellow color of gold is a result of low bandgap between contracted s and expanded d orbital.[31] It is shown that the nonrelativistic energies of 5s and 4d orbitals of Ag are approximately the same as energies of nonrelativistic 6s and 5d orbitals of Au respectively in AgH and AuH molecules as an example, but when one consider reletevistic effects, energy enhancement of 6S orbital and energy reduction of $5d_{5/2}$ and $5d_{3/2}$ spinors of Au are higher than energy enhancement of 5S orbital and energy reduction of $4d_{5/2}$ and $4d_{3/2}$ of Ag respectively, which result in "golden" color of Au and "silvery" color of Ag.[32, 33] In case of Cu, this relativistic effect is weaker in comparison with Ag, due to its lighter nucleus (relativistic mass (m)/nonrelativistic mass(m_0)) for Cu, Ag and Au is 1.023, 1.064 and 1.22 respectively[3]). The 5d to Fermi level transition energy for Au metal is about 2.3 eV, so it can absorb blue and green part of visible spectrum and looks golden. Light absorption of Ag is in 3.5 eV (in UV region), so reflect visible spectrum.[32] The reddish color of Cu is independent of relativistic effects and is due to 3d-4s transition energy, which is about 1.8-2.0 eV, so it also absorbs yellow and looks red.

1 Q. Jiang, X. Sheng, B. Shi, X. Feng and T. Xu, *J. Phys. Chem. B*, 2014, **118**, 25878–25883.

2 Y. Kato, L. K. Ono, M. V. Lee, S. Wang, S. R. Raga and Y. Qi, *Adv. Mater. Interfaces*, 2015, **2**, 1500195.

3 K. Hwang, Y. S. Jung, Y. J. Heo, F. H. Scholes, S. E. Watkins, J. Subbiah, D. J. Jones, D. Y. Kim and D. Vak, *Adv. Mater.*, 2015, **27**, 1241–1247.

4 J. H. Kim, S. T. Williams, N. Cho, C. Chueh and A. K. Jen, *Adv. Energy Mater.*, 2015, **5**.

5 K. Hwang, Y. Jung, Y. Heo, F. H. Scholes, S. E. Watkins, J. Subbiah, D. J. Jones, D. Kim and D. Vak, *Adv Mater*, 2015, **27**, 1241–1247.

6 Q. Lin, A. Armin, R. Chandra, R. Nagiri, P. L. Burn and P. Meredith, 2015, **9**, 106–112.

7 Y. Li, L. Meng, Y. M. Yang, G. Xu, Z. Hong, Q. Chen, J. You, G. Li, Y. Yang and Y. Li, *Nat. Commun.*, 2016, **7**, 10214.

8 D. Liu and T. L. Kelly, *Nat. Photonics*, 2014, **8**, 133–138.

9 S. Sun, T. Salim, N. Mathews, M. Duchamp, C. Boothroyd, G. Xing, T. C. Sum and Y. M. Lam, *Energy Environ. Sci.*, 2014, **7**, 399–407.

10 X. Zhou, C. Bao, F. Li, H. Gao, T. Yu, J. Yang, W. Zhu and Z. Zou, *RSC Adv.*, 2015, **5**, 58543–58548.

11 I. Jeong, H. J. Kim, B. Lee, H. J. Son, J. Y. Kim, D. Lee, D. Kim, J. Lee, M. J. Ko, I. Jeong, H. J. Kim, B. Lee, H. J. Son, J. Y. Kim, D. Lee, D. Kim, J. Lee and M. J. Ko, *Nano Energy*, 2015, **17**.

12 B. A. Nejand, V. Ahmadi and H. R. Shahverdi, *ACS Appl. Mater. Interfaces*, 2015, **7**, 21807–21818.

13 D. Bryant, D., Greenwood, P., Troughton, J., Wijdekop, M., Carnie, M., Davies, M., Wojciechowski, K., Snaith, H., Watson T., Worsley, *Adv. Mater.*, 2014, 7499–7504.

14 M. Saliba, T. Matsui, J.-Y. Seo, K. Domanski, N. Correa-Baena, Juan-Pablo

12 B. A. Nejand, V. Ahmadi and H. R. Shahverdi, *ACS Appl. Mater. Interfaces*, 2015, **7**, 21807–21818.

13 D. Bryant, D., Greenwood, P., Troughton, J., Wijdekop, M., Carnie, M., Davies, M., Wojciechowski, K., Snaith, H., Watson T., Worsley, *Adv. Mater.*, 2014, 7499–7504.

14 M. Saliba, T. Matsui, J.-Y. Seo, K. Domanski, N. Correa-Baena, Juan-Pablo Mohammad K., S. M. Zakeeruddin, W. Tress, A. Abate, A. Hagfeldt and M. Gratzel, *Energy Environ. Sci.*, 2016.

15 Y. Luo, X. Chen, C. Zhang, J. Li, J. Shi, Z. Sun, Z. Wang and S. Huang, *RSC Adv.*, 2015, **5**, 56037–56044.

16 D. Bryant, P. Greenwood, J. Troughton, M. Wijdekop, M. Carnie, M. Davies, K. Wojciechowski, H. J. Snaith, T. Watson and D. Worsley, *Adv. Mater.*, 2014, **26**, 7499–7504.

17 Z. Li, S. A. Kulkarni, P. P. Boix, E. Shi, A. Cao, K. Fu, S. K. Batabyal, J. Zhang, Q. Xiong, L. H. Wong, N. Mathews and S. G. Mhaisalkar, *ACS Nano*, 2014, **8**, 6797–6804.

18 Z. Wei, K. Yan, H. Chen, Y. Yi, T. Zhang, X. Long, J. Li, L. Zhang, J. Wang and S. Yang, *Energy Environ. Sci.*, 2014, **7**, 3326–3333.

19 D. Wang, Z. Liu, Z. Zhou, H. Zhu, Y. Zhou, C. Huang, Z. Wang, H. Xu, Y. Jin, B. Fan, S. Pang and G. Cui, *Chem. Mater.*, 2014, 141124013805002.

20 Y. Deng, Q. Dong, C. Bi, Y. Yuan and J. Huang, *Adv. Energy Mater.*, 2016.

21 E. M. Miller, Y. Zhao, C. C. Mercado, S. K. Saha, J. M. Luther, K. Zhu, V. Stevanović, C. L. Perkins and J. van de Lagemaat, *Phys. Chem. Chem. Phys.*, 2014, **16**, 22122–22130.

22 A. Dymshits, A. Henning, G. Segev, Y. Rosenwaks and L. Etgar, *Sci. Rep.*, 2015, **5**, 8704.

23 K.-G. Lim, S. Ahn, Y.-H. Kim, Y. Qi and T.-W. Lee, *Energy Environ. Sci.*, 2016, **9**, 932–939.

24 X. Liu, C. Wang, L. Lyu, C. Wang, Z. Xiao, C. Bi, J. Huang and Y. Gao, *Phys. Chem. Chem. Phys.*, 2014, **17**, 896–902.

25 J. Kim, S. H. Lee, J. H. Lee and K. H. Hong, *J. Phys. Chem. Lett.*, 2014, **5**, 1312–1317.

26 W. Yin, T. Shi and Y. Yan, *Appl. Phys. Lett.*, 2014, **104**, 063903.

27 K. Miyano, N. Tripathi, M. Yanagida and Y. Shirai, *Acc. Chem. Res.*, 2016, acs.accounts.5b00436.

28 A. Walsh, D. O. Scanlon, S. Chen, X. G. Gong and S. Wei, 2015,1791–1794.

29 X. Liu, C. C. Wang, L. Lyu, C. C. Wang, Z. Xiao, C. Bi, J. Huang and Y. Gao, *Phys. Chem. Chem. Phys.*, 2014, **17**, 896–902.

30 C. Quarti, E. Mosconi and F. De Angelis, *Chem. Mater.*, 2014, **26**, 6557–6569.

31 N. E. Christensen and B. O. Seraphin, 1971, 4.

32 P. Pyykko and J. P. Desclaux, Acc. Chem. Res., 1979, **12**, 276–281.

33 J. S. Thayer, Relativistic Methods for Chemists, Springer science, 2010, vol. 0172 .

29 X. Liu, C. C. Wang, L. Lyu, C. C. Wang, Z. Xiao, C. Bi, J. Huang and Y. Gao, *Phys. Chem. Chem. Phys.*, 2014, **17**, 896–902.

30 C. Quarti, E. Mosconi and F. De Angelis, *Chem. Mater.*, 2014, **26**, 6557–6569.